Stability of localized structures in generalized DNLS equations near the anti-continuum limit

2009 J. Phys. A: Math. Theor. 42 025207

(http://iopscience.iop.org/1751-8121/42/2/025207)

J. Phys. A: Math. Theor. **42** (2009) 025207 (13pp) doi:10.1088/1751-8113/42/2/025207

Stability of localized structures in generalized DNLS equations near the anti-continuum limit

V M Rothos[1], H E Nistazakis[2], P G Kevrekidis[3] and D J Frantzeskakis[2]

[1] Department of Mathematics, Physics Computational Sciences, Faculty of Engineering, Aristotle University of Thessaloniki, Thessaloniki 54124, Greece
[2] Department of Physics, University of Athens, Panepistimiopolis, Zografos, Athens 15784, Greece
[3] Department of Mathematics and Statistics, University of Massachusetts, Amherst, MA 01003-4515, USA

Received 27 August 2008, in final form 24 October 2008
Published 4 December 2008
Online at stacks.iop.org/JPhysA/42/025207

Abstract
In this work we consider the stability of localized structures in discrete nonlinear Schrödinger lattices with generalized nonlinearities, depending on the absolute value of the field. We illustrate how the continuation of solutions in one-, as well as higher dimensions proceeds from the anti-continuum limit and show how to generalize the results of Pelinovsky *et al* (2005 *Physica* D **212** 1) for arbitrary nonlinearities. As a case example of particular experimental relevance, we showcase our main findings in the special setting of the lattice with the saturable (photorefractive) nonlinearity in one and two dimensions. Our analytical results are found to be in good agreement with direct numerical computations.

PACS number: 05.45.Yv
Mathematics Subject Classification: 34K20, 37K60, 47B39

1. Introduction

Over the past decade, dynamical lattice problems, especially of Hamiltonian dispersive type have become relevant for a diverse host of applications from different areas of physics. One of the principal areas that have led to numerous insights has been the nonlinear optics of fabricated AlGaAs waveguide arrays [1]. In that setting, the interplay of discreteness and nonlinearity led to the emergence of many interesting phenomena including, for instance, Peierls–Nabarro potential barriers, diffraction and diffraction management [2], gap solitons [3] and so on (see also the reviews [5, 6] and references therein). Perhaps, the most prototypical mathematical model used in the description of such waveguide arrays is the discrete nonlinear Schrödinger (DNLS) equation [11].

A more recent development in the area of nonlinear optics that has been a focal point for theoretical, computational and experimental developments has been the proposal and creation of optically induced photonic lattices in photorefractive crystals such as strontium barium

niobate (SBN). After the original theoretical proposition of these lattices [12], experimental realizations soon followed [13, 14], paving the way for the observation of an array of exciting nonlinear wave phenomena in such crystals. One can mention, among many others, the formation of patterns such as dipole [15], quadrupole [16] and necklace [17] solitary waves, impurity modes [18], discrete vortices [19, 20], rotary waves [21], higher order Bloch modes [22] and gap vortices [23], two-dimensional (2D) Bloch oscillations and Landau–Zener tunneling [24], the formation of coherent structures in honeycomb [25], hexagonal [26] and quasi-crystalline lattices [27], and most recently the study of Anderson localization in disordered photonic lattices [28]. An interesting deviation of this class of photorefractive problems from the standard DNLS setting is that the nonlinearity does not have the regular cubic form, representing the Kerr effect, but rather has a saturable functional form, representative of the photorefractive nonlinearity. This feature will be of importance in our considerations below.

Finally, yet another physical realization of such lattices emerged in recent years in atomic physics through the examination of Bose–Einstein condensates (BECs) trapped in periodic potentials. There, again, a reduction can be formulated which is obtained as an effective description of the mean-field model of the so-called Gross–Pitaevskii equation with a periodic potential. This leads once again to a genuinely discrete nonlinear Schrödinger equation [7].

The above physical realizations have prompted an extensive examination of the coherent structures that emerge in the prototypical dispersive nonlinear lattice dynamical model, namely the DNLS equation; see, e.g., [8–10] for one-, two- and three-dimensional installments of the model, as well as references therein. However, there is a considerably smaller volume of such results for non-cubic nonlinearities, such as for instance the saturable nonlinearity of the photorefractive media, or the cubic–quintic nonlinearity. Recently, the existence of intrinsic localized modes in DNLS with saturable nonlinearity has been proved rigorously using the Nehari manifolds approach and a mountain pass argument [4]. The saturable case has been examined predominantly due to some of its interesting stability properties (such as the exchange of stability between the on-site and the inter-site solitary wave modes) [30, 31] and the related possibility for potentially enhanced mobility of localized lattice excitations [31]. The cubic-quintic case has been studied due to a larger variety of localized modes that it can offer and its richer bifurcation structure [32, 33].

In the present work, our aim is to present a theory for the localized excitations in the vicinity of the anti-continuum limit (where the sites are decoupled from each other) in the case of generalized DNLS models, where the nonlinearity is an arbitrary function of the field modulus. This situation encompasses, as case examples, the photorefractive nonlinearity (in which we test these predictions in detail), as well as the cubic–quintic case, and generalizes in a natural way the earlier results of [8, 9].

This paper is structured as follows. In section 2, we present the mathematical formulation of the problem and the theoretical results of linear stability analysis. In section 3, we present numerical results for the existence and linear stability of discrete breathers (in the 1D setting) and vortices (in the 2D setting) of the DNLS equation with saturable nonlinearity. Finally, section 4 presents our conclusions.

2. Mathematical analysis

2.1. Formulation of the problem

We start by considering the generalized DNLS equation of the form:

$$\mathrm{i}\dot{u}_n + F(|u_n|^2)(u_{n+1} + u_{n-1}) + f(u_n, \bar{u}_n) = 0, \qquad n \in \mathbb{Z}, \quad t \in \mathbb{R}. \tag{2.1}$$

The nonlinear functions F, f will be assumed to be polynomial functions of their arguments with real coefficients. In addition, it is useful to take $F(\rho) > 0$ for all $\rho > 0$ and $f = g(|u_n|^2)u_n$. There are several choices one can make for the functions F, g such that the system (2.1) has the NLS-type equation as a continuum limit:

(a) $F(\rho) = \varepsilon$ and $g(\rho) = -2\varepsilon + a_1\rho$, $g(\rho) = -2\varepsilon + a_1/(1+\rho)$, $g(\rho) = -2\varepsilon + a_1\rho - \rho^2$. These correspond to the cubic DNLS, saturable DNLS and cubic–quintic DNLS models, respectively, discussed in the introduction.
(b) $F(\rho) = \varepsilon + a_1\rho/3$ and $g(\rho) = -2\varepsilon + a_1\rho/3$. This corresponds to the so-called Salerno model [34]; see also [35] for some recent considerations regarding this model.
(c) $F(\rho) = \varepsilon + a_1\rho/2$ and $g = -2\varepsilon$. This corresponds to the Ablowitz–Ladik model which is the integrable counterpart of the DNLS equation [29].

In the following sections, as per the discussion in the introduction, we focus on case A, where $\varepsilon > 0$ and $a_1 = 1$ (focusing case). It should be noted that the results can be straightforwardly translated to the defocusing case of $\varepsilon < 0$ through the, so-called, staggering transformation $\tilde{u}_n = (-1)^n u_n$.

Let

$$l^2 = \left\{ u = \{u_n\}_{n\in\mathbb{Z}},\, u_n \in \mathbb{C},\, \|u\| = \left(\sum_{n\in\mathbb{Z}} |u|^2 \right)^{1/2} \right\}$$

with the real scalar product

$$\langle \phi, \psi \rangle_{l^2} = \mathrm{Re} \sum_n \phi_n \bar{\psi}_n, \qquad \psi, \psi \in l^2.$$

Considering the discrete Laplacian operator we observe that for any $\phi \in l^2$:

$$\|\Delta\phi\|_{l^2}^2 \leqslant 4\|\phi\|_{l^2}^2.$$

We rewrite the equation in the form

$$\mathrm{i}\dot{u}_n + \varepsilon\Delta u_n + f(u_n, \bar{u}_n) = 0 \tag{2.2}$$

and $\Delta u_n := u_{n+1} - 2u_n + u_{n-1}$.

The discrete breathers of (2.2) are given by

$$u_n(t) = \phi_n \, \mathrm{e}^{\mathrm{i}(\mu - 2\varepsilon)t + \mathrm{i}\theta_0}, \qquad \mu \in \mathbb{R}, \quad \phi_n \in \mathbb{C}, \quad n \in \mathbb{Z}, \tag{2.3}$$

where $\theta_0 \in \mathbb{R}$ is a parameter and (μ, ϕ_n) solve the difference equation on $n \in \mathbb{Z}$:

$$(\mu - g(|\phi_n|^2))\phi_n = \varepsilon(\phi_{n+1} + \phi_{n-1}). \tag{2.4}$$

Proposition 1. *Choosing $\mu = \mu_*$, where $\mu_* = 1$ for the cubic DNLS and $\mu_* = 1/2$ for the saturable DNLS, there exist $\varepsilon_0 > 0, \kappa > 0, \phi_\infty > 0$ such that the difference equation (2.4) has a continuous family of intrinsic localized modes near the anti-continuum limit of $\varepsilon = 0$, with the properties:*

(i)

$$\lim_{\varepsilon\to 0^+} \phi_n = \phi_n^{(0)} = \begin{cases} \mathrm{e}^{\mathrm{i}\theta_n}, & n \in \mathbb{S} \\ 0, & n \in \mathbb{Z}\backslash\mathbb{S} \end{cases} \tag{2.5}$$

(ii)

$$\lim_{|n|\to\infty} \mathrm{e}^{\kappa|n|}\phi_n = \phi_\infty, \qquad \phi_n \in \mathbb{R}, \qquad n \in \mathbb{Z}, \tag{2.6}$$

where $\mathbb{S}$ is a finite set of nodes of the lattice $n \in \mathbb{Z}$ and $\theta_n = \{0, \pi\}$, $n \in \mathbb{S}$.

The difference equations can be rewritten as

$$(\mu_* - g(|\phi_n|^2))\phi_n = \varepsilon(\phi_{n+1} + \phi_{n-1}). \tag{2.7}$$

For the solution of the equation, given the analyticity of the vector field equations on ϵ, one can use the perturbative expansion

$$\phi_n = \phi_n^{(0)} + \sum_{k=1}^{\infty} \varepsilon^k \phi_n^{(k)}, \tag{2.8}$$

$\phi_n^{(0)}$ is given by (2.5). Following Pelinovsky *et al* [8] we have:

Lemma 1. *There exists* $0 < \varepsilon_1 < \varepsilon_0$ *such that the number of changes in the sign of* ϕ_n *on* $n \in \mathbb{Z}$ *for* $0 < \varepsilon < \varepsilon_1$ *is equal to the number of* π*-differences of the adjacent* θ_n, $n \in \mathbb{S}$, *in the limiting solution (2.5).*

By proposition 1 and lemma 1, all families of the discrete breathers as $\varepsilon \to 0$ can be classified by a sequence of $\{0\}$, $\{+\}$ and $\{-\}$ of the limiting solution (2.5) on the finite set $\mathbb{S}$. In particular, we consider two ordered sets $\mathbb{S}$:

$$\mathbb{S}_1 = \{1, 2, 3, \ldots, N\} \tag{2.9}$$

and

$$\mathbb{S}_2 = \{1, 3, 5, \ldots, 2N-1\}, \tag{2.10}$$

where $\dim(\mathbb{S}_1) = \dim(\mathbb{S}_2) = N < \infty$. The set $\mathbb{S}_1$ includes the, so-called, Page mode ($N = 2, \theta_1 = \theta_2 = 0$) and the twisted mode ($N = 2, \theta_1 = 0, \theta_2 = \pi$). The set $\mathbb{S}_2$ includes the Page and twisted modes ($N = 2$), separated by an empty node.

2.2. *Stability of discrete breathers*

The spectral stability of discrete breathers for DNLS with saturable nonlinearity is studied through the linearization

$$u_n(t) = \mathrm{e}^{\mathrm{i}(\mu_* - 2\varepsilon)t + \mathrm{i}\theta_0}(\phi_n + a_n \mathrm{e}^{\lambda t} + \bar{b}_n \mathrm{e}^{\bar{\lambda} t}), \tag{2.11}$$

where $\lambda \in \mathbb{C}$, $(a_n, b_n) \in \mathbb{C}^2$ solve the linear problem on $n \in \mathbb{Z}$,

$$\begin{aligned} &\left(\mu_* - \frac{\partial f}{\partial u_n}\right) a_n - \frac{\partial f}{\partial \bar{u}_n} b_n - \varepsilon(a_{n+1} + a_{n-1}) = \mathrm{i}\lambda a_n \\ &-\frac{\bar{\partial} f}{\partial \bar{u}_n} a_n + \left(\mu_* - \frac{\bar{\partial} f}{\partial u_n}\right) b_n - \varepsilon(b_{n+1} + b_{n-1}) = -\mathrm{i}\lambda b_n. \end{aligned} \tag{2.12}$$

Focusing on real profiles ϕ_n and substituting $a_n = u_n + \mathrm{i}w_n, b_n = u_n - \mathrm{i}w_n$ the stability problem (2.12) is transformed to

$$\begin{aligned} &\left(\mu_* - \left(\frac{\partial f}{\partial v_n} + \frac{\partial f}{\partial \bar{v}_n}\right)\right) v_n - \varepsilon(v_{n+1} + v_{n-1}) = -\lambda w_n \\ &\left(\mu_* - \left(\frac{\partial f}{\partial v_n} - \frac{\partial f}{\partial \bar{v}_n}\right)\right) w_n - \varepsilon(w_{n+1} + w_{n-1}) = \lambda v_n. \end{aligned} \tag{2.13}$$

The matrix–vector form of the problem (2.13) is

$$\mathcal{L}_+ \boldsymbol{v} = -\lambda \mathbf{w}, \qquad \mathcal{L}_- \mathbf{w} = \lambda \boldsymbol{v} \tag{2.14}$$

where if we use $f(u_n, \bar{u}_n) = g(|u_n|^2)u_n$

$$\begin{aligned}(\mathcal{L}_+)_{n,n} &= \mu_* - \left[\left(\frac{\partial g}{\partial u_n} + \frac{\partial g}{\partial \bar{u}_n}\right)u_n + g\right],\\ (\mathcal{L}_-)_{n,n} &= \mu_* - \left[\left(\frac{\partial g}{\partial u_n} - \frac{\partial g}{\partial \bar{u}_n}\right)u_n + g\right],\\ (\mathcal{L}_\pm)_{n,n+1} &= (\mathcal{L}_\pm)_{n+1,n} = -\varepsilon\end{aligned} \tag{2.15}$$

Equivalently, the stability problem is rewritten in the Hamiltonian form

$$\mathcal{J}\mathcal{H}\psi = \lambda\psi, \tag{2.16}$$

where ψ is the infinite-dimensional eigenvector that consists of 2-blocks of $(v_n, w_n)^T$, $\mathcal{J}$ is the infinite-dimensional skew-symmetric matrix that consists of 2×2 blocks of

$$\mathcal{J}_{n,m} = \begin{pmatrix} 0 & 1 \\ -1 & 0 \end{pmatrix}\delta_{n,m}$$

and $\mathcal{H}$ is the infinite-dimensional symmetric matrix that consists of 2×2 blocks of

$$\mathcal{H} = \begin{pmatrix} (\mathcal{L}_+)_{n,m} & 0 \\ 0 & (\mathcal{L}_-)_{n,m} \end{pmatrix}.$$

Due to (2.8), the matrix $\mathcal{H}$ is expanded into the power series

$$\mathcal{H} = \mathcal{H}^{(0)} + \sum_{k=1}^{\infty} \varepsilon^k \mathcal{H}^{(k)} \tag{2.17}$$

where $\mathcal{H}^{(0)}$ is diagonal with the block elements:

$$\begin{aligned}\mathcal{H}^{(0)}_{n,n} &= \begin{pmatrix} (\mathcal{L}_+)_{n,n}|_{\phi_n^{(0)}} & 0 \\ 0 & (\mathcal{L}_-)_{n,n}|_{\phi_n^{(0)}} \end{pmatrix} \qquad n \in \mathbb{S},\\ \mathcal{H}^{(0)}_{n,n} &= \begin{pmatrix} \mu_* & 0 \\ 0 & \mu_* \end{pmatrix}, \qquad n \in \mathbb{Z}\backslash\mathbb{S}.\end{aligned} \tag{2.18}$$

Let $N = \dim(\mathbb{S}) < \infty$. For $\varepsilon = 0$, the spectrum of $\mathcal{H}^{(0)}\varphi = \gamma\varphi$ has exactly N eigenvalues

$$\gamma = (\mathcal{L}_+)_{n,n}|_{\phi_n^{(0)}},$$

N zero eigenvalues $\gamma = 0$ and infinitely many eigenvalues $\gamma = \mu_* - g(0)$. The eigenvalues

$$\gamma = (\mathcal{L}_+)_{n,n}|_{\phi_n^{(0)}} \qquad \text{and} \qquad \gamma = 0$$

map to N double zero eigenvalues $\lambda = 0$ in the eigenvalue problem $\mathcal{J}\mathcal{H}^{(0)}\psi = \lambda\psi$. The remaining infinitely many eigenvalues map to the infinitely many eigenvalue pairs $\lambda = \pm i(\mu_* - g(0))$ for the full problem.

We can prove the following lemma:

Lemma 2. *Assume that $\phi_n, n \in \mathbb{Z}$ is the discrete breather, described in proposition 1. Let $N = \dim(\mathbb{S}) < \infty$. Let $\gamma_j, 1 \leqslant j \leqslant N$, be small eigenvalues of $\mathcal{H}$ as $\varepsilon \to 0$ such that*

$$\lim_{\varepsilon\to 0} \gamma_j = 0, \qquad 1 \leqslant j \leqslant N. \tag{2.19}$$

There exists $0 < \varepsilon_* \leqslant \varepsilon_0$ such that the eigenvalue problem (2.16) with $\phi_n, n \in \mathbb{Z}$ and $0 < \varepsilon_* \leqslant \varepsilon_0$ has N pairs of small eigenvalues $\pm\lambda_j, 1 \leqslant j \leqslant N$, that satisfy the leading-order behavior

$$\lim_{\varepsilon\to 0} \frac{\lambda_j^2}{\gamma_j} = -(\mathcal{L}_+)_{n,n}|_{\phi_n^{(0)}}, \qquad 1 \leqslant j \leqslant N. \tag{2.20}$$

For the saturable DNLS with $\mu_* = 1/2$, $\mathcal{H}^{(0)}$ is diagonal with two blocks:

$$\mathcal{H}^{(0)}_{n,n} = \begin{pmatrix} -1/2 & 0 \\ 0 & 0 \end{pmatrix}, \qquad n \in \mathbb{S}, \qquad \mathcal{H}^{(0)}_{n,n} = \begin{pmatrix} -1/2 & 0 \\ 0 & -1/2 \end{pmatrix}, \qquad n \in \mathbb{Z}\backslash\mathbb{S}. \quad (2.21)$$

Let $N = \dim(\mathbb{S}) < \infty$. The spectrum of $\mathcal{H}^{(0)}\varphi = \gamma\varphi$ has N zero eigenvalues and infinitely many eigenvalues $\gamma = -1/2$. Among these the N zero eigenvalues, along with N of the $-1/2$ eigenvalues map to N double zero eigenvalues of the full problem, while the remaining infinite eigenvalues of $-1/2$ map to the eigenvalues $\lambda = \pm i/2$.

For the models of type A considered herein, the calculation of the small eigenvalues γ_j proceeds in a similar way as in [8] and is provided by a reduced eigenvalue problem

$$\mathcal{M}_j \mathbf{c} = \gamma_j \mathbf{c}, \quad (2.22)$$

where $\mathbf{c} = (c_1, \ldots, c_N)^\top$ is the corresponding eigenvector and $\mathcal{M}_j$ a tri-diagonal $N \times N$ matrix, given by equation:

$$\begin{aligned} &(\mathcal{M}_j)_{n,n} = (\cos(\theta_{n+1} - \theta_n) + \cos(\theta_{n-1} - \theta_n)), \qquad 1 < n < N \\ &(\mathcal{M}_j)_{n,n+1} = (\mathcal{M}_j)_{n+1,n} = -\cos(\theta_{n+1} - \theta_n), \qquad 1 < n < N \\ &(\mathcal{M}_j)_{1,1} = \cos(\theta_2 - \theta_1), \qquad (\mathcal{M}_j)_{N,N} = \cos(\theta_N - \theta_{N-1}). \end{aligned} \quad (2.23)$$

It can be shown by a calculation analogous to that of [8] that in the case of the nearest-neighbor excited sites of the set $\mathbb{S}_1$, the relevant order of emergence of the small eigenvalues is $j = 1$ and the full problem eigenvalues are $\lambda = \sqrt{\epsilon}\lambda_1$, while if the sites are next-nearest neighbor as in $\mathbb{S}_2$, then the relevant order is $j = 2$, and the eigenvalues are $\lambda = \epsilon\lambda_2$. We now test these predictions by means of direct numerical bifurcation computations.

3. Numerical stability analysis

3.1. Discrete breathers in the 1D saturable model

In this section, as a prototypical example of a non-cubic nonlinearity (as well as one which is of fundamental interest in its own right due to its connection with the properties of photorefractive media), we present a numerical analysis of the existence and linear stability results associated with the DNLS equation with saturable nonlinearity. We examine the stability with two examples of the discrete breathers in the set $\mathbb{S}_1$: $N = 2$ and $N = 3$. In the case $N = 2$ the discrete two-pulse breathers consist of the in-phase mode (a) and the, so-called, twisted [36, 37] or out-of-phase mode (b) as follows:

$$\begin{aligned} &(a) \quad \theta_1 = \theta_2 = 0 \\ &(b) \quad \theta_1 = 0, \qquad \theta_2 = \pi. \end{aligned} \quad (3.1)$$

The eigenvalues of matrix $\mathcal{M}_1$ are given explicitly as $\gamma_1 = 0$ and $\gamma_2 = 2\cos(\theta_2 - \theta_1)$. Therefore, the in-phase mode (a) has one unstable eigenvalue $\lambda \approx \sqrt{\epsilon}$ in the stability problem (2.16) for small $\epsilon > 0$, while the twisted mode (b) has no unstable eigenmodes but rather only a simple pair of purely imaginary eigenvalues $\lambda \approx \pm i\sqrt{\epsilon}$ with the so-called negative Krein signature; see [8] for a definition of the Krein signature and a proof of its negativity which holds true also in the present context. These results are illustrated in figures 1 and 2 in agreement with the numerical computations of the full linearization equations (2.7) and (2.12). Figure 1 shows the in-phase mode, while figure 2 corresponds to the twisted mode. The top subplots of each figure illustrate the mode profile (left) and the spectral plane $\lambda = \lambda_r + i\lambda_i$ of the linear eigenvalue problem (right) for $\epsilon = 0.1$. The bottom subplot indicates the corresponding real (for the in-phase mode) and imaginary (for the twisted mode) eigenvalues from the theory (dashed line) versus the full numerical result (solid line). We found that the agreement between the theory and the numerical computation is within 5% for $\epsilon < 0.0665$ in the in-phase case

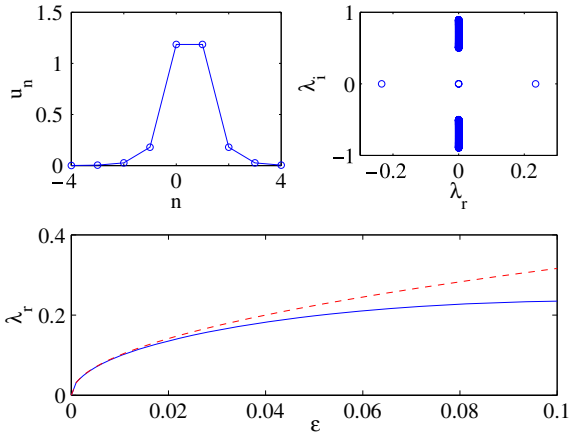

Figure 1. The top left panel shows the spatial profile of two in-phase excited sites while the top right panel shows the corresponding spectral plane of the linear stability problem for $\epsilon = 0.1$. The bottom panel shows the theoretically (dashed line) and the numerically (solid line) evaluated real positive eigenvalue, from $\epsilon = 0$ to $\epsilon = 0.1$.

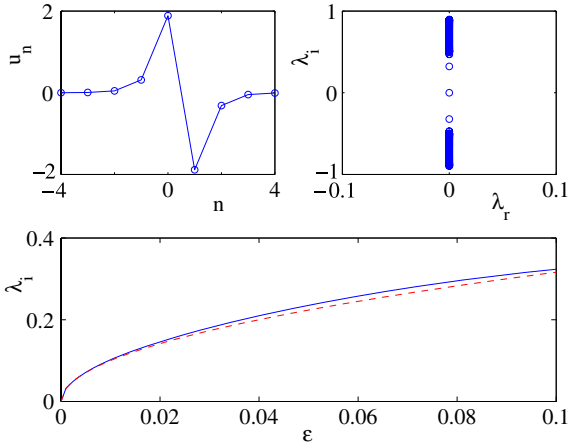

Figure 2. Same as figure 1 but now for the twisted mode with two out-of-phase excited sites.

(figure 1), while for the twisted mode (figure 2) it is less than 1.5% for all the values of ϵ in the interval $(0, 0.1)$. As may naturally be anticipated, for larger values of ϵ the difference between the theory and the numerics grows since higher order terms of the perturbative expansion for the eigenvalues come into play. In the case $N = 3$, the discrete three-pulse breathers consist of three principal modes as follows:

$$\begin{aligned} &(a) \quad \theta_1 = \theta_2 = \theta_3 = 0 \\ &(b) \quad \theta_1 = \theta_2 = 0, \qquad \theta_3 = \pi \\ &(c) \quad \theta_1 = 0, \qquad \theta_2 = \pi, \qquad \theta_3 = 0. \end{aligned} \tag{3.2}$$

The eigenvalues of matrix $\mathcal{M}_1$ are given explicitly as $\gamma_1 = 0$ and

$$\gamma_{2,3} = \cos(\theta_2 - \theta_1) + \cos(\theta_3 - \theta_2) \pm \sqrt{\cos^2(\theta_2 - \theta_1) - \cos(\theta_2 - \theta_1)\cos(\theta_3 - \theta_2) + \cos^2(\theta_3 - \theta_2)}.$$

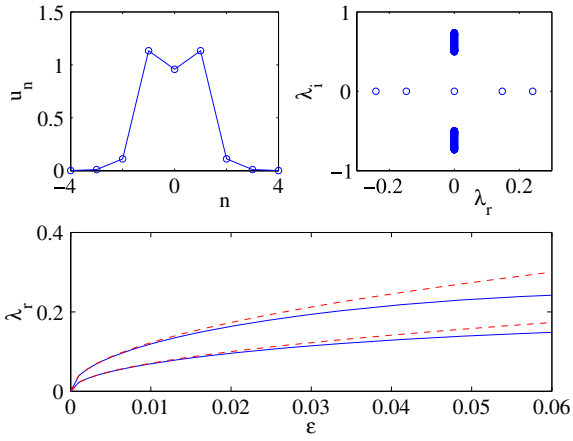

Figure 3. Same as figure 1 but for three excited sites in phase. In the top panels the spatial profile and the corresponding spectral plane of the linear stability problem are shown for $\epsilon = 0.06$.

The mode (a) has two real unstable eigenvalues $\lambda \approx \sqrt{3\epsilon/2}$ and $\lambda \approx \sqrt{\epsilon/2}$ in the stability problem (2.16). The mode (b) has one real unstable eigenvalue $\lambda \approx \sqrt{\sqrt{3}\epsilon/2}$ and a simple pair of purely imaginary eigenvalues $\lambda \approx \pm i\sqrt{\sqrt{3}\epsilon/2}$ with negative Krein signature. The mode (c) has no unstable eigenvalues but two pairs of purely imaginary eigenvalues $\lambda \approx \pm i\sqrt{3\epsilon/2}$ and $\lambda \approx \pm i\sqrt{\epsilon/2}$ with negative Krein signature. Figures 3–5 summarize the results of the three modes (a)–(c), given in (3.2). Figure 3 corresponds to the in-phase mode (a), where two real positive eigenvalues give rise to the instability for any $\epsilon \neq 0$. The error between the theoretical and numerical results is within 5% for $\epsilon < 0.0524$ for one real eigenvalue while for the other it is smaller than 3.5% for every ϵ in the interval $(0, 0.06)$. Similar results are observed in figure 4 for the mode (b), where the real positive eigenvalue and a pair of imaginary eigenvalues with negative Krein signature are generated for $\epsilon > 0$. Finally, figure 5 shows the mode (c), where two pairs of imaginary eigenvalues with negative Krein signature exist for positive ϵ. In both cases of the modes (b) and (c), the error between the theoretical and numerical results is within 5% for every value of ϵ in the interval $[0, 0.1]$.

It is interesting to compare the results from the above analysis with the equivalent from the case of cubic nonlinearity [8]. It is straightforward to establish that since the eigenvalues γ_j in all considered cases are identical between the cubic and saturable models, and since $(\mathcal{L}_+)_{n,n}\big|^{(\text{cubic})}_{\phi_n^{(0)}} = 4(\mathcal{L}_+)_{n,n}\big|^{(\text{saturable})}_{\phi_n^{(0)}}$, the relevant eigenvalues of the cubic case will be a factor of 2 larger than their corresponding saturable counterparts (for the values of μ in the two models considered herein which yield the same excited mode intensities). This implies the following: for a given ϵ, structures that are unstable due to the existence of real eigenvalues will be less unstable in the saturable model than their analogues in the cubic model. On the other hand, structures with imaginary eigenvalues of negative Krein signature in the saturable model possess a wider (in ϵ) stability interval than pertinent ones in the cubic model. These results illustrate the advantages of constructing waveguide arrays in media with photorefractive or photovoltaic nonlinearities instead of Kerr ones; similar conclusions have been drawn, in fact, for dark solitons in the defocusing case in connection with experiments (see, e.g., [38] and references therein).

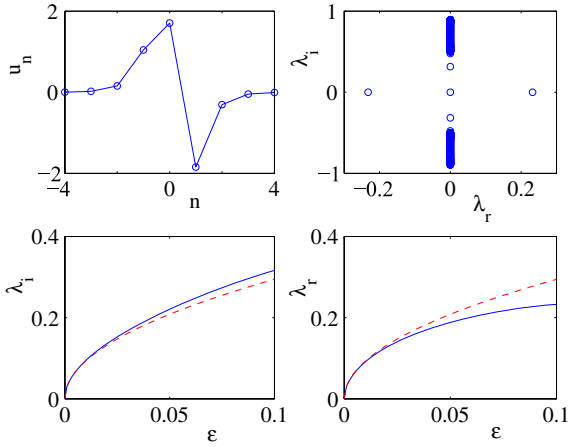

Figure 4. Same as figure 1 but for three excited sites where the left and the middle sites are in phase and the right is out of phase. The top panels are for $\epsilon = 0.1$.

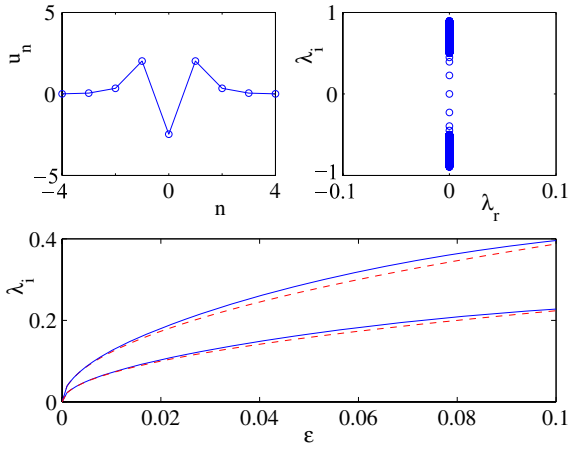

Figure 5. Same as figure 4 but for three excited sites where adjacent sites are out of phase with each other.

3.2. Discrete vortices in the 2D saturable model

We now turn to the case of the model with the saturable nonlinearity in two spatial dimensions [11], which we also briefly consider to illustrate the generality of our results above.

$$\mathrm{i}\dot{u}_{n,m} + \epsilon(u_{n+1,m} + u_{n-1,m} + u_{n,m+1} + u_{n,m-1} - 4u_{n,m}) + \frac{u_{n,m}}{1 + |u_{n,m}|^2} = 0, \tag{3.3}$$

where $u_{n,m}(t)$:$\mathbb{R}_+ \to \mathbb{C}$, $(n, m) \in \mathbb{Z}^2$, and $\epsilon > 0$ is the inverse squared step size of the lattice. The discrete NLS conserves the (squared) l^2 norm which corresponds to the, so-called, optical power:

$$Q = \sum_{(n,m)\in\mathbb{Z}^2} |u_{n,m}|^2. \tag{3.4}$$

The conservation of power is related to the invariance of the discrete NLS (3.3) with respect to the gauge transformation:

$$u_{n,m}(t) \mapsto u_{n,m}(t)\, e^{i\theta_0}, \qquad \forall\, \theta_0 \in \mathbb{R}. \tag{3.5}$$

The time periodic localized modes of the two-dimensional discrete NLS equation take the form

$$u_{n,m}(t) = \phi_{n,m}\, e^{i(\mu-4\varepsilon)t+i\theta_0}, \qquad \phi_{n,m} \in \mathbb{C} \tag{3.6}$$

where $\theta_0 \in \mathbb{R}$ and $\mu \in \mathbb{R}$ are parameters. The localized modes in the focusing discrete NLS with $\epsilon > 0$ exist only for $\mu > 4\epsilon$ [39]. The parameter $\mu > 0$ can be set as $\mu = 1/2$ and the complex-valued $\phi_{n,m}$ solve the nonlinear difference equations on $(n, m) \in \mathbb{Z}^2$:

$$\left(\frac{1}{2} - \frac{1}{1+|\phi_{n,m}|^2}\right)\phi_{n,m} = \varepsilon(\phi_{n+1,m} + \phi_{n-1,m} + \phi_{n,m+1} + \phi_{n,m-1}). \tag{3.7}$$

If $\epsilon = 0$, the localized modes of the equation (3.7) are given by the following limiting solution:

$$\phi^{(0)}_{n,m} = \begin{Bmatrix} e^{i\theta_{n,m}}, & (n,m) \in \mathbb{S} \\ 0, & (n,m) \in \mathbb{Z}^2 \backslash \mathbb{S} \end{Bmatrix} \tag{3.8}$$

where $\mathbb{S}$ is a finite set of nodes of the lattice $(n, m) \in \mathbb{Z}^2$ and $\theta_{n,m}$ is the parameter for $(n, m) \in \mathbb{S}$. The value of θ_0 is arbitrary in the ansatz (3.6), so we can set $\theta_{n_0,m_0} = 0$ for the node $(n_0, m_0) \in \mathbb{S}$. This convention allows us to precisely define a special type of localized mode, the vortex, which can be given as follows [9]. If $\mathbb{S}$ is a simple closed discrete contour on the plane $(n, m) \in \mathbb{Z}^2$, the localized solution of the differential equations (3.7) with $\epsilon > 0$, which has complex-valued $\phi_{n,m}$ and satisfies the limit (3.8) with $\theta_{n,m} \in [0, 2\pi]$, $(n, m) \in \mathbb{S}$, is called a discrete vortex. Additionally, each node $(n, m) \in \mathbb{S}$ has exactly two adjacent nodes in the vertical or horizontal directions along $\mathbb{S}$. $\Delta\theta_j$ is the phase difference between two adjacent nodes in $\mathbb{S}$, with $j = 1, 2, \ldots, \dim(\mathbb{S})$ and $|\Delta\theta_j| \leqslant \pi$. If the phase differences $\Delta\theta_j$ are constant along $\mathbb{S}$, the discrete vortex is called symmetric and if not, asymmetric. The total number of 2π phase shifts across the closed contour $\mathbb{S}$ is called the vortex charge. If $|\Delta\theta_j| \in \{0, \pi\}$, then the solution is called a discrete breather, while if it does not belong to this set, then the solution is called a (genuine) discrete vortex. We consider the square discrete contour $S = S_M$:

$$\begin{aligned} S_M = \{&(1,1), \ldots, (M+1,1), (M+1,2), \ldots, \\ &(M+1, M+1), (M, M+1), \ldots, (1, M+1), \ldots, (1,2)\} \end{aligned} \tag{3.9}$$

and the dimension of S_M is $4M$. As mentioned above, the contour S_M for fixed M can support symmetric and asymmetric vortices with charge L. The simplest vortex is symmetric with charge one ($M = 1, L = 1$) [40, 41]. To showcase a prototypical example of the generality of our approach developed above, in this work we will investigate the stability of symmetric vortices [9] where their charge, L, is not equal to the size of the contour M[4]. The particular case of interest that we will study is one of the cases of most physical interest, i.e. with $M = 2$ and $L = 3$; this case is quite relevant for the contour with $M = 2$ since it is the lowest charge for which the configuration is stable near the anti-continuum limit [9]. The contour S_M for $M = 2$ is shown in figure 6. The values of $\theta_{i,j}$ with $i, j = 1, 2, 3$ are $\theta_{1,1} = 0$, $\theta_{2,1} = 3\pi/4$, $\theta_{3,1} = 3\pi/2$, $\theta_{3,2} = 9\pi/4$, $\theta_{3,3} = 3\pi$, $\theta_{2,3} = 15\pi/4$, $\theta_{1,3} = 9\pi/2$, $\theta_{1,2} = 21\pi/4$.

The spectral stability of the discrete vortices (3.6) with $\mu = 1/2$ and $\theta_0 = 0$ is studied, similarly to the case of the 1D DNLS equation (since the closed contour considered corresponds

[4] For the case of $L = M$, higher order reductions need to be developed similarly to [9].

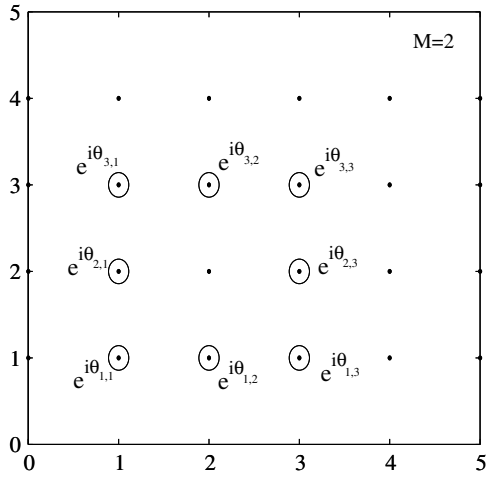

Figure 6. Example of close square contour S_M for $M = 2$.

effectively to a 1D configuration with periodic boundary conditions). The linearization around such structures reads:

$$u_{n,m}(t) = e^{i(1/2-4\varepsilon)t+i\theta_0}(\phi_{n,m} + a_{n,m}\, e^{\lambda t} + \bar{b}_{n,m}\, e^{\bar{\lambda} t}), \tag{3.10}$$

where $\lambda \in \mathbb{C}$ and $(a_n, b_n) \in \mathbb{C}^2$. For the cases of non-super-symmetric vortices, i.e., $L \neq M$, the method developed above for the 1D DNLS case based on the leading-order expansions generalizes to 2D settings on appropriate contours [9]. For the example of interest in this case of the charge $L = 3$ vortex for the 8-site contour with $M = 2$, where the relative phase between adjacent sites is $3\pi/4$ we can again use the Jacobian matrix of equation (2.23). One can then derive the following eigenvalue predictions:

$$\lambda = \sqrt{2\epsilon \cos(\Delta\theta)} \sin\left(\frac{\pi n}{N}\right) \qquad n = 1, 2, \ldots, N, \tag{3.11}$$

where the number of sites is $N = 8$ and $\Delta\theta = 2\pi L/N = 3\pi/4$. The results from equation (3.11) are tested in the numerical bifurcation calculations presented in figure 7. The first-order reductions predict three pairs of double imaginary eigenvalues for $n = 1, 2, 3$ and $n = 5, 6, 7$,

$$\lambda = \pm i\sqrt{\sqrt{2}\epsilon} \sin\left(\frac{\pi n}{N}\right), \tag{3.12}$$

a pair of simple imaginary eigenvalues for $n = 4$,

$$\lambda = \pm i\sqrt{\sqrt{2}\epsilon} \tag{3.13}$$

and a double zero eigenvalue for $n = 8$ (due to the overall phase invariance). The double non-zero eigenvalues split into the second-order reductions along the imaginary axis (with negative Krein signature). Nevertheless, the qualitative description of the above formula is, in fact, correct and the results are even quantitatively accurate for small ε (i.e., for values smaller than 0.005), in which interval the second-order corrections are weak. In figure 7, we give both the leading order prediction and the full numerical result for the seven relevant pairs of eigenvalues. Note once again that the relevant saturable mode eigenvalues are predicted to be half of their cubic case counterparts. This illustrates once again (for the same mode intensity and the same coupling) the more stable nature (or wider parametric interval of stability) of the coherent structures in the former model.

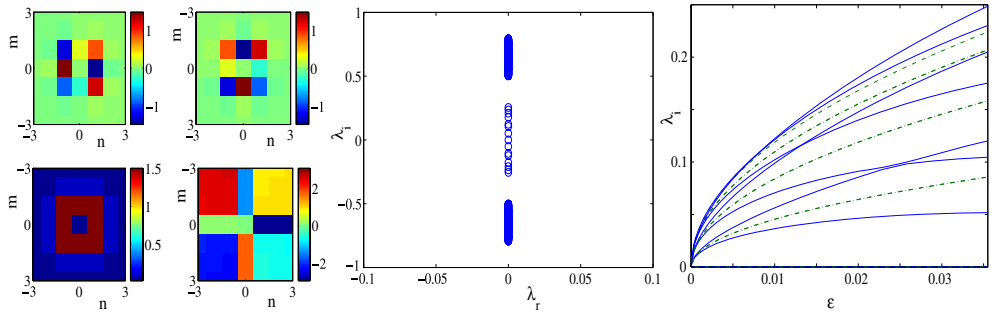

Figure 7. The vortex cell with $L = 3$ and $M = 2$. The left panel shows the profile of the solution for $\epsilon = 0.0354$. The subplots show the real (top left), imaginary (top right), modulus (bottom left) and phase (bottom right) fields. The middle panel shows the spectral plane (λ_r, λ_i) of the linear eigenvalue problem. The right panel shows the numerically (solid line) and theoretically (dashed line) evaluated, through the first-order reduction, imaginary eigenvalues versus ϵ, for values between $\epsilon = 0$ and $\epsilon = 0.0354$.

4. Conclusions

In this work, we considered generalized DNLS models where the nonlinearity is not necessarily cubic but can assume any form dependent on the field and its complex conjugate. We showed how to generalize in this case the considerations of [8, 9] and obtain explicit expressions for the eigenvalues of both one-dimensional configurations and discrete breathers, as well as two-dimensional configurations and discrete vortices, in the vicinity of the anti-continuous limit where the sites are uncoupled with each other. The results were shown to be in excellent qualitative and good quantitative agreement with the full numerical stability results in the case example of the saturable nonlinearity, relevant to the photorefractive media. A physically relevant conclusion that we were able to deduce from these considerations was that for structures of the same intensity and coupling strength, the relevant eigenvalues in the saturable model are smaller than their counterparts in the cubic model. This suggests that the structures are either less unstable or have a wider parametric interval of stability in the saturable case, in comparison with the cubic one.

There are a number of directions along which it would be relevant/interesting to extend the present considerations. A natural one is the extension of the present findings to either higher-dimensional configurations (such as three-dimensional ones, analogously to the very recent work of [10]), or multi-component ones (similarly to [42]). Perhaps a more mathematically challenging, yet equally interesting direction would be to extend the present considerations to settings that do not involve only simple linear coupling between nearest neighbors, but perhaps also include nonlinear variants thereof (similar to the ones present in the Salerno or Ablowitz-Ladik models). Developing a general theory for the latter would enable a toolbox that could address any member of the DNLS family which would be a valuable contribution for present and potential future purposes/applications of such models. Efforts along these directions are currently in progress and will be reported in future publications.

Acknowledgments

PGK gratefully acknowledges support from NSF-DMS-0505663, 0619492, 0806762 and NSF-CAREER, as well as from the Alexander von Humboldt foundation. The work of DJF was partially supported by the Special Research Account of the University of Athens.

References

[1] Eisenberg H S, Silberberg Y, Morandotti R, Boyd A R and Aitchison J S 1998 *Phys. Rev. Lett.* **81** 3383
[2] Morandotti R, Peschel U, Aitchison J S, Eisenberg H S and Silberberg Y 1999 *Phys. Rev. Lett.* **83** 2726–9
Eisenberg H S, Silberberg Y, Morandotti R and Aitchison J S 2000 *Phys. Rev. Lett.* **85** 1863
[3] Mandelik D, Morandotti R, Aitchison J S and Silberberg Y 2004 *Phys. Rev. Lett.* **92** 093904
[4] Pankov A and Rothos V 2008 Periodic and decaying solutions in DNLS with saturable nonlinearity *Proc. R. Soc. London* A **464** 3219
[5] Christodoulides D N, Lederer F and Silberberg Y 2003 *Nature* **424** 817–23
Sukhorukov A A, Kivshar Yu S, Eisenberg H S and Silberberg Y 2003 *IEEE J. Quantum Elect.* **39** 31
[6] Aubry S 1997 *Physica* **103D** 201
Flach S and Willis C R 1998 *Phys. Rep.* **295** 181
[7] Kevrekidis P G, Frantzeskakis D J and Carretero-González R (ed) 2008 *Emergent Nonlinear Phenomena in Bose-Einstein Condensates: Theory and Experiment* (Heidelberg: Springer)
[8] Pelinovsky D E, Kevrekidis P G and Frantzeskakis D J 2005 *Physica* D **212** 1
[9] Pelinovsky D E, Kevrekidis P G and Frantzeskakis D J 2005 *Physica* D **212** 20
[10] Lukas M, Pelinovsky D and Kevrekidis P G 2008 *Physica* D **237** 339
[11] Kevrekidis P G, Rasmussen K O and Bishop A R 2001 *Int. J. Mod. Phys.* B **15** 2833
[12] Efremidis N K, Sears S, Christodoulides D N, Fleischer J W and Segev M 2002 *Phys. Rev.* E **66** 46602
[13] Fleischer J W, Segev M, Efremidis N K and Christodoulides D N 2003 *Nature* **422** 147
[14] Fleischer J W, Carmon T, Segev M, Efremidis N K and Christodoulides D N 2003 *Phys. Rev. Lett.* **90** 023902
[15] Yang J, Makasyuk I, Bezryadina A and Chen Z 2004 *Opt. Lett.* **29** 1662
[16] Yang J, Makasyuk I, Bezryadina A and Chen Z 2004 *Stud. Appl. Math.* **113** 389
[17] Yang J, Makasyuk I, Kevrekidis P G, Martin H, Malomed B A, Frantzeskakis D J and Chen Z 2005 *Phys. Rev. Lett.* **94** 113902
[18] Fedele F, Yang J and Chen Z 2005 *Opt. Lett.* **30** 1506
[19] Neshev D N, Alexander T J, Ostrovskaya E A, Kivshar Yu S, Martin H, Makasyuk I and Chen Z 2004 *Phys. Rev. Lett.* **92** 123903
[20] Fleischer J W, Bartal G, Cohen O, Manela O, Segev M, Hudock J and Christodoulides D N 2004 *Phys. Rev. Lett.* **92** 123904
[21] Kartashov Y V, Vysloukh V A and Torner L 2004 *Phys. Rev. Lett.* **93** 093904
Wang X, Chen Z and Kevrekidis P G 2006 *Phys. Rev. Lett.* **96** 083904
[22] Träger D, Fischer R, Neshev D N, Sukhorukov A A, Denz C, Królikowski W and Kivshar Yu S 2006 *Optics Express* **14** 1913
[23] Bartal G, Manela O, Cohen O, Fleischer J W and Segev M 2005 *Phys. Rev. Lett.* **95** 053904
[24] Trompeter H, Królikowski W, Neshev D N, Desyatnikov A S, Sukhorukov A A, Kivshar Yu S, Pertsch T, Peschel U and Lederer F 2006 *Phys. Rev. Lett.* **96** 053903
[25] Peleg O, Freedman G Bartal B, Manela O, Segev M and Christodoulides D N 2007 *Phys. Rev. Lett.* **98** 103901
[26] Rosberg C R, Neshev D N, Sukhorukov A A, Krolikowski W and Kivshar Yu S 2007 *Opt. Lett.* **32** 397
[27] Freedman B, Bartal G, Segev M, Lifshitz R, Christodoulides D N and Fleischer J W 2006 *Nature* **440** 1166
[28] Schwartz T, Bartal G, Fishman S and Segev M 2007 *Nature* **446** 52
[29] Berger A, MacKay R S and Rothos V M 2004 *Discr. Cont. Dyn. Syst.* B **4** 911
[30] Hadzievski L, Maluckov A, Stepić M and Kip D 2004 *Phys. Rev. Lett.* **93** 033901
[31] Melvin T R O, Champneys A R, Kevrekidis P G and Cuevas J 2006 *Phys. Rev. Lett.* **97** 124101
[32] Carretero-González R, Talley J D, Chong C and Malomed B A 2006 *Physica* D **216** 77
[33] Chong C, Carretero-González R, Malomed B A and Kevrekidis P G 2008 *Preprint* arXiv:0805.0497
[34] Salerno M 1992 *Phys. Rev.* A **46** 6856
[35] Pelinovsky D E, Melvin T R O and Champneys A R 2007 *Physica* D **236** 22
[36] Darmanyan S, Kobyakov A and Lederer F 1998 *Sov. Phys.—JETP* **86** 682
[37] Kevrekidis P G, Bishop A R and Rasmussen K O 2001 *Phys. Rev.* E **63** 036603
[38] Fitrakis E P, Kevrekidis P G, Susanto H and Frantzeskakis D J 2007 *Phys. Rev.* E **75** 066608
[39] Hennig D and Tsironis G 1999 *Phys. Rep.* **307** 333
[40] Malomed B A and Kevrekidis P G 2001 *Phys. Rev.* E **64** 026601
[41] Yang J and Musslimani Z 2003 *Opt. Lett.* **28** 2094
[42] Kevrekidis P G and Pelinovsky D E 2006 *Proc. R. Soc. London* A **462** 2671